

Supplementary information for:

THE CRYSTAL STRUCTURE OF BACTERIOPHAGE λ REXA PROVIDES NOVEL INSIGHTS INTO THE DNA BINDING PROPERTIES OF REX-LIKE PHAGE EXCLUSION PROTEINS

AUTHORS

Myfanwy C. Adams^{1†}, Carl J. Schiltz^{1†}, Jing Sun¹, Christopher J. Hosford¹, Virginia M. Johnson¹, Hao Pan¹, Peter P. Borbat^{2,3}, Jack H. Freed^{2,3}, Lynn C. Thomason⁴, Carolyn Court⁴, Donald L. Court⁴, and Joshua S. Chappie^{1,*}

¹ Department of Molecular Medicine, Cornell University, Ithaca, NY, 14853, USA

² Department of Chemistry and Chemical Biology, Cornell University, Ithaca, 14853, USA

³ National Biomedical Resource for Advanced Electron Spin Resonance Spectroscopy, Cornell University, Ithaca, 14853, USA

⁴ Center for Cancer Research, National Cancer Institute, Frederick, MD, 21702, USA

* To whom correspondence should be addressed. Tel: +1 (607) 253-3654; Fax: +1 (607) 253-3659; Email: chappie@cornell.edu

† These authors contributed equally

Present Address: Myfanwy C. Adams, John Innes Centre, Norwich Research Park, Norwich, UK

Present Address: Carl J. Schiltz, IDEXX Laboratories, Westbrook, ME, 04092, USA

Present Address: Jing Sun, Harvard University, Cambridge, MA 02140, USA

Present Address: Christopher J. Hosford, LifeMine Therapeutics, Cambridge, MA 02140, USA

Present Address: Virginia M. Johnson, Crop Science Division, Bayer, St. Louis, MO, 63141 USA

Present Address: Hao Pan, Sanofi, Waltham, MA 02451, USA

Supplementary Tables

Supplementary Table S1. X-ray data collection and refinement statistics.

Supplementary Table S2. Sequences of oligonucleotide substrates.

Supplementary Table S3. Dissociation constants from EMSA experiments.

Supplementary Table S4. *E. coli* K12 strains used for exclusion and papillation assays.

Supplementary statistical analysis of papillation data

Supplementary Figures

Supplementary Figure S1. Organization and regulation of the λ immunity region. Related to Figures 1 and 6.

Supplementary Figure S2. Location of RexA mutants. Related to Figures 1 and 4.

Supplementary Figure S3. Structural coordination of bound ions and sulfates. Related to Figure 1.

Supplementary Figure S4. Structure and topology of *E. coli* RdgC. Related to Figure 2.

Supplementary Figure S5. Additional structural homologies identified by Dali. Related to Figures 1, 2, and 3.

Supplementary Figure S6. Sequence alignment of putative RexA homologs. Related to Figures 3, 4, and 5.

Supplementary Figure S7. SEC analysis of RexA mutants. Related to Figures 4, 5, and 6.

Supplementary Figure S8. ESR spectroscopy measurements for D168C. Related to Figure 5.

Supplementary Figure S9. Gene neighborhoods surrounding RexA-like genes in Actinobacteriophages. Related to Figure 7.

Supplementary Figure S10. Sequence alignment of unique RexA-like proteins present in Actinobacteriophage viruses. Related to Figure 7.

Supplementary Figure S11. SEC analysis of purified RexA homologs. Related to Figure 7.

Supplementary Figure S12. Comparison of operator sequences used in binding experiments. Related to Figures 4, 5, and 7.

Supplementary Figure S13. AlphaFold model of Toast gp42 and comparison to RexA. Related to Figures 3 and 7.

Supplementary Table S1. X-ray data collection and refinement statistics.

	RexA SeMet Crystal form 1	RexA SeMet Crystal form 2 PDB: 8TWQ
Data collection		
Space group	P32 2 1	P32 2 1
Cell dimensions		
<i>a</i> , <i>b</i> , <i>c</i> (Å)	56.4, 56.4, 326.22	55.65, 55.65, 322.12
α , β , γ (°)	90, 90, 120	90, 90, 120
Resolution (Å)	108.74 – 2.68 (2.81 – 2.68)	161.06 – 2.05 (2.11 – 2.05)
<i>R</i> _{sym} or <i>R</i> _{merge}	0.127 (0.913)	0.118 (0.931)
<i>R</i> _{meas}	0.132 (0.997)	0.128 (1.010)
<i>CC</i> _{1/2} (%)	0.997 (0.634)	0.998 (0.595)
<i>I</i> / σI	14.2 (1.7)	13.4 (1.9)
Completeness (%)	100.0 (100.0)	99.9 (100.0)
Redundancy	8.9 (8.0)	6.8 (6.6)
Phasing		
Initial F.O.M.	0.3	
Number of sites	14	
Refinement		
Resolution (Å)		53.69 – 2.05
No. reflections		37768 (3651)
<i>R</i> _{work} / <i>R</i> _{free} (%)		0.2063 / 0.2512
No. atoms		4637
Protein		4367
Ligand/ion		49
Water		221
<i>B</i> -factors		37.46
Protein		37.24
Ligand/ion		58.93
Water		37.18
R.m.s deviations		
Bond lengths (Å)		0.0009
Bond angles (°)		1.04
Ramachandran statistics		
Favored (%)		92.86
Allowed (%)		6.04
Outliers (%)		1.10

*Values in parentheses are for highest-resolution shell. Each dataset was derived from a single crystal.

Supplementary Table S2. Sequences of oligonucleotide substrates.

Oligonucleotide	Sequence
EMSA_02_US	5'- CCACTGGCGGTGAT -3'
EMSA_02*_US	5'- (6-FAM) – CCACTGGCGGTGAT -3'
EMSA_02_LS	5'- ATCACC GCCAGTGG -3'
Rex_OR1-OR2_US	5'- CATTATCACCGCCAGAGGTAAATAGTCAACACGCACGGTGTTAGAT -3'
Rex_OR1-OR2_LS	5'- ATCTAACACCGTGCGTGTTGACTATTTTACCTCTGGCGGTGATAATG -3'
Rex_OR1-OR2_Scram_US	5'- CATGCCAGGATATTCGCTACAAATAGTACGTGATACGACATCGCGAT -3'
Rex_OR1-OR2_Scram_LS	5'- ATCGCGATGTCGTATCACGTACTATTTGTAGCGAATATCCTGGCATG -3'
Toast_OR1-OR2-OR3_US	5'- CACCGACCCGGCTACCGCTTAACGCGTGTCGTGTCGCACCTGCCGTCTAC CAATGACTACCGGGGATTGTGCCTCATATCCGCAGGCTGCGGAACCTACAG GGCTGTAATTTCTTGACGAGCGTCTACCTGCTGCGGAAGAATCATCCGCA GCCTATTGACACCACCCCGTCTACCAGGAGAGACTCATG -3'
Toast_OR1-OR2-OR3_LS	5 - CATGAGTCTCTCCTGGTAGACGGGGTGGTGTCAATAGGCTGCGGATGATT CTTCCGCAGCAGGTAGACGCTCGTCAAGAAATTACAGCCCTGTAGTTCCG CAGCCTGCGGATATGAGGCACAATCCCCGGTAGTCATTGGTAGACGGCA GGTGCGACACGACACGCGTTAAGCGGTAGCCGGGTCGGTG -3'
Sbash_OR1-OR2-OR3_US	5'- CATACGTCGAGTCTGACAGAAACATTTCGGCAAACCTTTGAACTGGGTGGC AAACATCATCAGTGTAATTTCTCCGACTATTGGGTCTTAGGTCAAGAAAC CCCTGGTAGTCCAGGTTTGCCGTTTTAGGAAAAGTTTCGGCATGTGGTTT GCCGACCCGAATCTACGGTGTATCTTCGGGGATATG -3'
Sbash_OR1-OR2-OR3_LS	5'- CATATCCCCGAAGATACACCGTAGATTCGGGTCGGCAAACCGACATGCCG AACTTTTCTAAACCGGCAAACCTGGACTACCAGGGGTTTCTTGACCTAA GACCCAATAGTCGGAGGAAATTACACTGATGATGTTTGCCACCCAGTTG AAAGTTTGCCGAATGTTTCTGTCAGACTCGACGTATG -3'
CarolAnn_OR1-OR2-OR3_US	5'- CATGGATTGAGGTTCAACCGCCCGTCCTTCGGCACGCAACGCGCAACGG AACCTATGCGGTTACCGCGTTTGCTCGCTCCGGCTTCCTTCTCCGTGTAC CAACTTGTCCCCGGATTGTGCCGCATACACGCAGGCTGCGGAACCTACCG CCGTGTAATTCATTGCCATGCGTGTACCCACCATGCAAGAATCATACGCAG TTGCTTGACACCCAGCCGTTACCGAGGAGGATCAATGGCGAGCTACACA CGCTGGCCGAAGGGAAGTTGGATG -3'
CarolAnn_OR1-OR2-OR3_LS	5'- CATCCAACCTTCCCTTCGGCCAGCGTGTGTAGCTCGCCATTGATCCTCCTC GGTAACCGGCTGGGTGTCAAGCAACTGCGTATGATTCTTGCATGGTGGGT ACACGCATGGCAATGAATTACACGGCGGTAGTTCCGCAGCCTGCGTGTAT GCGGCACAATCCGGGGGACAAGTTGGTACACGGAGAAGGAAGCCGGAGC GAGCAAACGCGGTAACCGCATAGGTTCCGTTGCGCGTTGCGTGCCGAAG GACGGGCGGTTGAACCTCAATCCATG -3'

Supplementary Table S3. Dissociation constants from EMSA experiments

	K_d (app) μM	+/- Std. Dev.
Figure 4		
WT	1.25	0.068
G140A	0.93	0.10
G140P	0.86	0.11
G140-K143>AAAA	ND	ND
Δ 239-244	7.94	0.48
D215W	0.14	0.0028
R219A/K221A	ND	ND
C258S/C269S/K2C	1.80	0.0095
Figure 7A – Lambda Operator (top row)		
Sbash30	3.50	1.80
CarolAnn44	7.02	1.00
Toast42	9.25	2.88
Figure 7B – Scrambled Lambda Operator (middle row)		
Sbash30	5.89	1.28
CarolAnn44	8.84	0.88
Toast42	10.10	2.80
Figure 7C – Cognate Operator (bottom row)		
Sbash30	0.68	0.19
CarolAnn44	0.24	0.0079
Toast42	0.85	0.024

All values represent the average of three independent EMSA experiments (see **MATERIALS AND METHODS** for details on K_d measurement and calculation). The oligonucleotide substrates used in each experiment are described in the respective figure legends with the sequences shown in **Supplementary Table S2**. 'ND' signifies 'not determined' due to incomplete saturation within the data acquisition range.

Supplementary Table S4. *E. coli* K12 strains used for exclusion and papillation assays.

Strain	Relevant Genotype	Reference/construction
LT351	MG1655	From B. Bochner
Cc3LT732	MG1655 <i>lacI</i> ^p <> <i>kan-Ter</i> <> <i>lac</i> <>'N <i>pLoL rexB rexA cI857 pRoR cro</i> '<> <i>lacZYA</i> ⁺	Thomason et al., (2019) (1)
LT772	MG1655 <i>lacI</i> ^p <> <i>kan-Ter</i> <> <i>lac</i> <>'N <i>pLoL (rexB rexA)</i> <> <i>cat cI857 pRoR cro</i> '<> <i>lacZYA</i> ⁺	This work
LT1055	MG1655 <i>ΔlacI-kan luc-N pLoL rexB</i> ⁺ <i>rexA</i> ⁺ <i>cI857ind1 pRoR cro27 cII-lacZYA</i> ⁺	Thomason et al., (2021) (2)
LT1886	MG1655 <i>ΔlacI-kan luc-N pLoL rexB</i> ⁺ <i>rexA</i> ⁺ <i>cI857 pRoR cro</i> ⁺ <i>cII-lacZYA</i> ⁺	Thomason et al. (2021) (2)
LT1892	MG1655 <i>ΔlacI-kan luc-N pLoL (rexB rexA)</i> <> <i>cat cI857 pRoR cro</i> ⁺ <i>cII-lacZYA</i> ⁺	Thomason et al. (2021) (2)
LT2294	MG1655 <i>ΔlacI-kan luc-N pLoL rexB</i> ⁺ <i>rexA(R219A/K221A) cI857 pRoR cro</i> ⁺ <i>cII-lacZYA</i> ⁺	This work
LT2298	MG1655 <i>ΔlacI-kan luc-N pLoL rexB</i> ⁺ <i>rexA(D215W) cI857 pRoR cro</i> ⁺ <i>cII-lacZYA</i> ⁺	This work
LT2299	MG1655 <i>ΔlacI-kan luc-N pLoL rexB</i> ⁺ <i>rexA(D215W) cI857 pRoR cro27 cII-lacZYA</i> ⁺	This work
LT2302	MG1655 <i>ΔlacI-kan luc-N pLoL rexB</i> ⁺ <i>rexA(Δ239-244) cI857 pRoR cro</i> ⁺ <i>cII-lacZYA</i> ⁺	This work
LT2303	MG1655 <i>ΔlacI-kan luc-N pLoL rexB</i> ⁺ <i>rexA(Δ239-244) cI857 pRoR cro27 cII-lacZYA</i> ⁺	This work

Supplementary statistical analysis of papillation data

For the data plotted in **Figure 6E**, t-tests were performed with GraphPad Prism software. In all cases, the number of papillae per colony observed with the *rexA* mutants was significantly different from that found with the wildtype RexA strains. For the Cro⁺ strains, both *rexA* mutants give fewer papillae than do wildtype RexA, while for the *cro27* strains, both *rexA* mutants give more papillae than does the wildtype RexA. When the two *rexA* mutants are compared to each other, in the Cro⁺ case there is no significant difference between them; however, for the *cro27* case, the two mutants are significantly different with D215W having more papillae/colony in a subset of the colonies. t-test values are as follows:

The difference in papillae/colony between LT1886 Cro⁺ RexA⁺ (M = 17.13; SD = 3.59) and LT2302 Cro⁺ *rexA* Δ239-244 (M = 13.32; SD = 4.42) was significant (t (207) = 6.804; p < <0.0001).

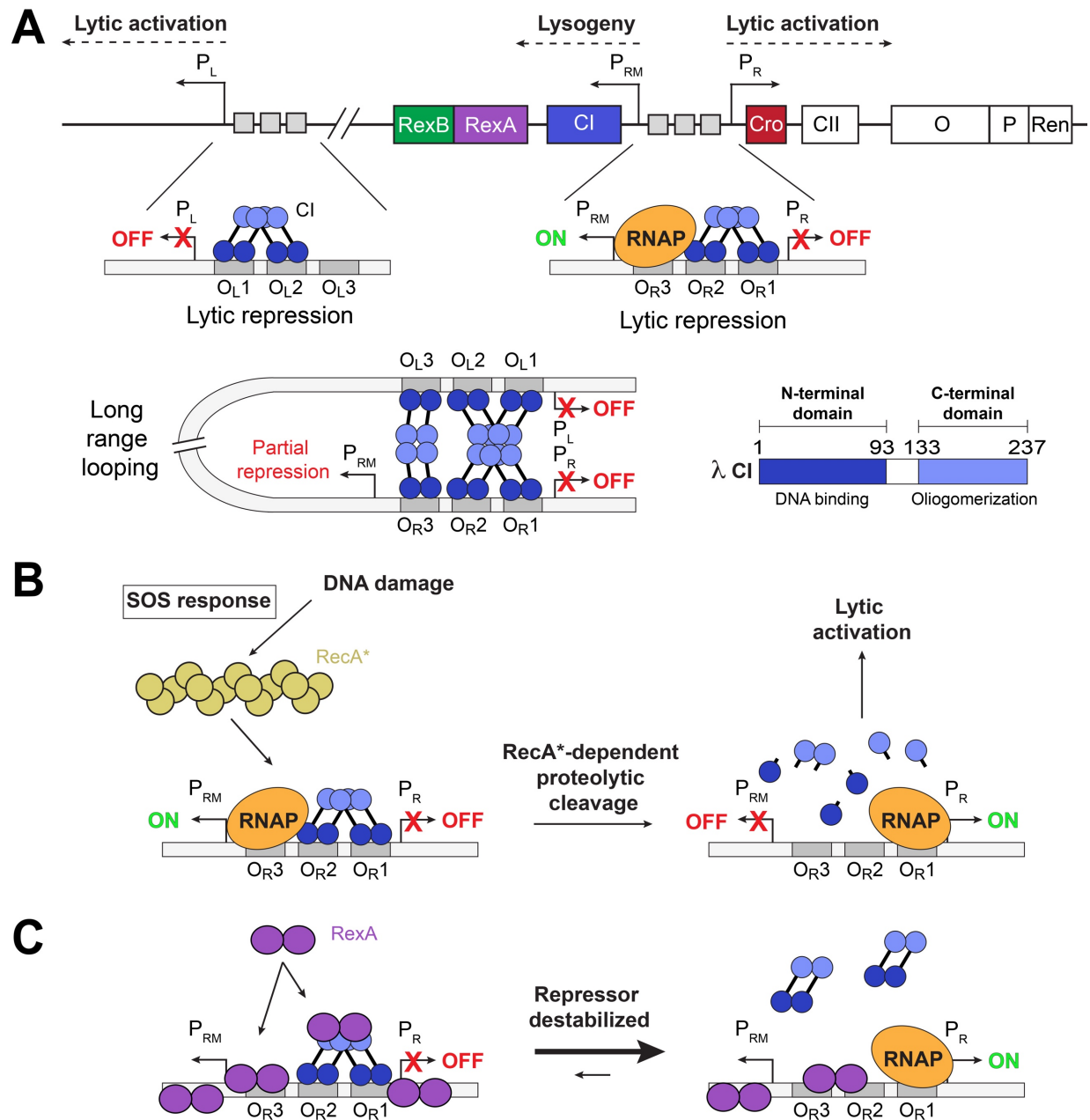
The difference in papillae/colony between LT1886 Cro⁺ RexA⁺ (M = 17.13; SD = 3.59) and LT2298 Cro⁺ *rexA* D215W (M = 14.56; SD = 4.78) was significant (t (202) = 4.332; p < 0.0001).

The difference in papillae/colony between LT1055 *cro27* RexA⁺ (M = 3.71; SD = 1.80) and LT2303 *cro27 rexA* Δ239-244 (M = 4.613; SD = 2.253) was significant (t (204) = 3.167; p < 0.0018).

The difference in papillae/colony between LT1055 *cro27* RexA⁺ (M = 3.71; SD = 1.80) and LT2299 *cro27 rexA* D215W (M = 9.234; SD = 7.313) was significant (t (205) = 7.347; p < 0.0001).

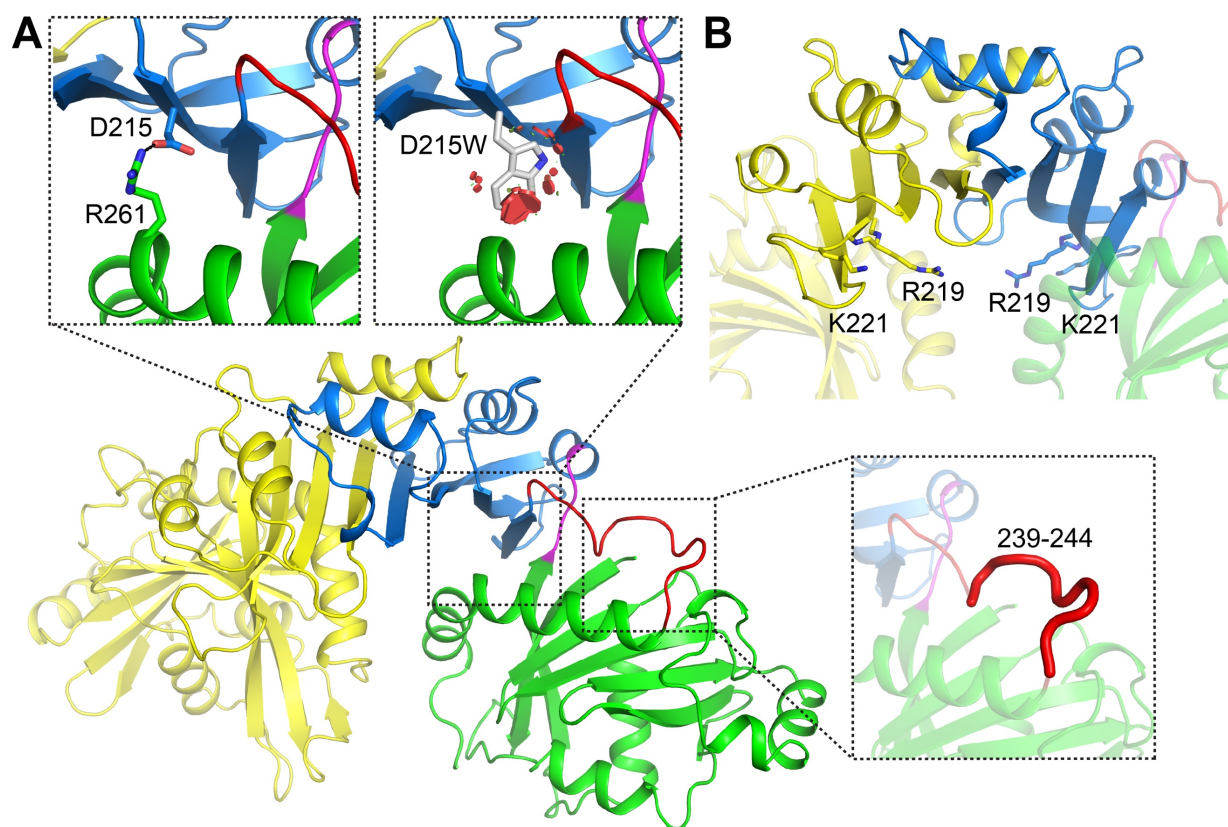
The difference in papillae/colony between LT2302 Cro⁺ *rexA* Δ239-244 (M = 13.32; SD = 4.42) and LT2298 Cro⁺ *rexA* D215W (M = 14.56; SD = 4.78) was not significant (t (211) = 1.962; p = 0.051).

The difference in papillae/colony between LT2303 *cro27 rexA* Δ239-244 (M = 4.613; SD = 2.253) and LT2299 *cro27 rexA* D215W (M = 9.234; SD = 7.313) was significant (t (211) = 6.219; p < 0.0001).

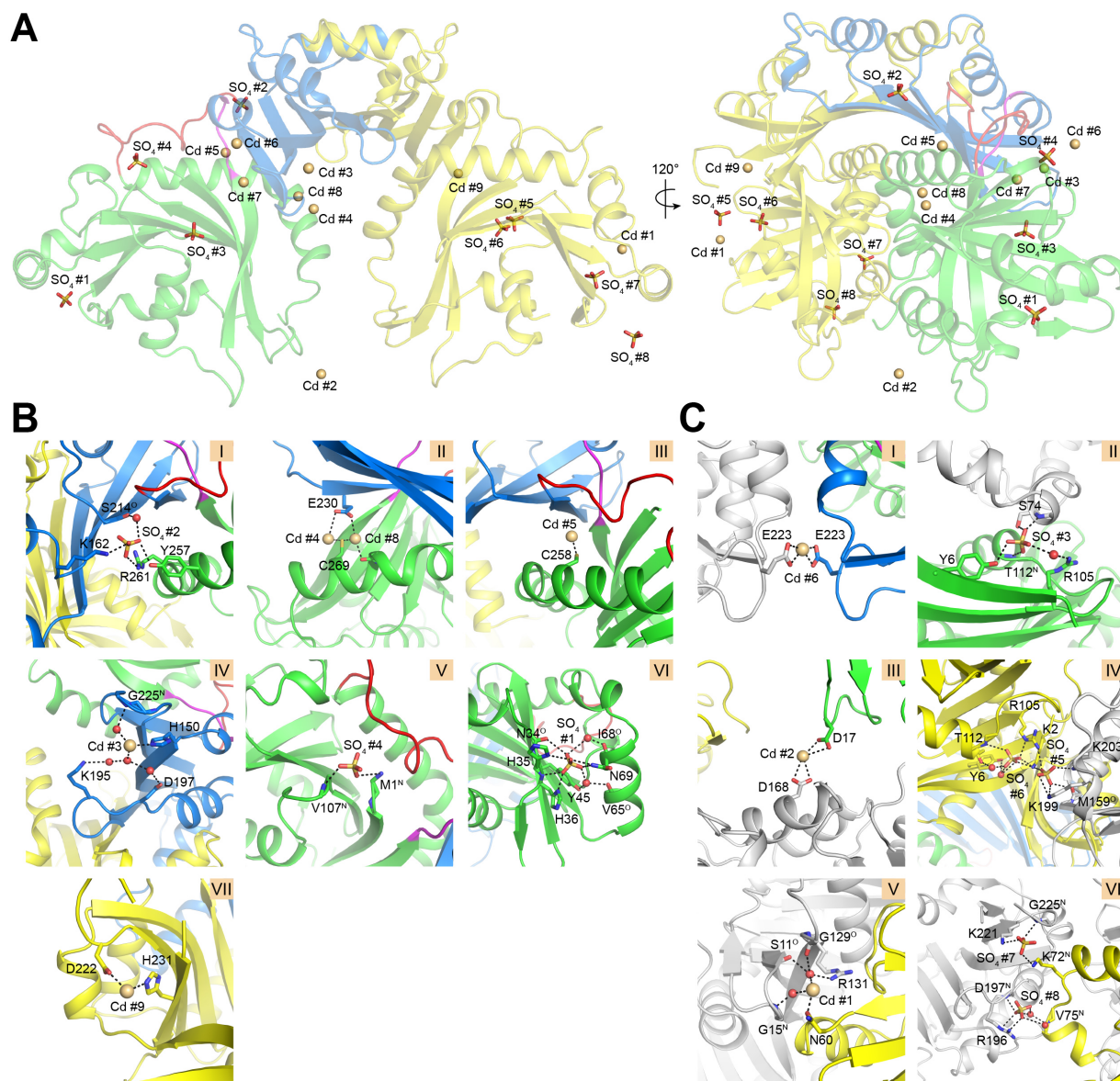


Supplementary Figure S1. Organization and regulation of the λ immunity region. A. Diagram of the λ immunity region. The positions of the P_L , P_{RM} and P_R promoters and neighboring genes are labeled. Associated operator sites are marked by gray boxes. In the lysogenic state, CI dimers (blue) are bound cooperatively to OL1 and OL2 and OR1 and OR2 operators to repress the lytic promoters P_L and P_R , respectively, and direct transcription from the maintenance promoter P_{RM} via RNA polymerase (RNAP, orange) (3, 4). Long-range DNA looping mediated by the further

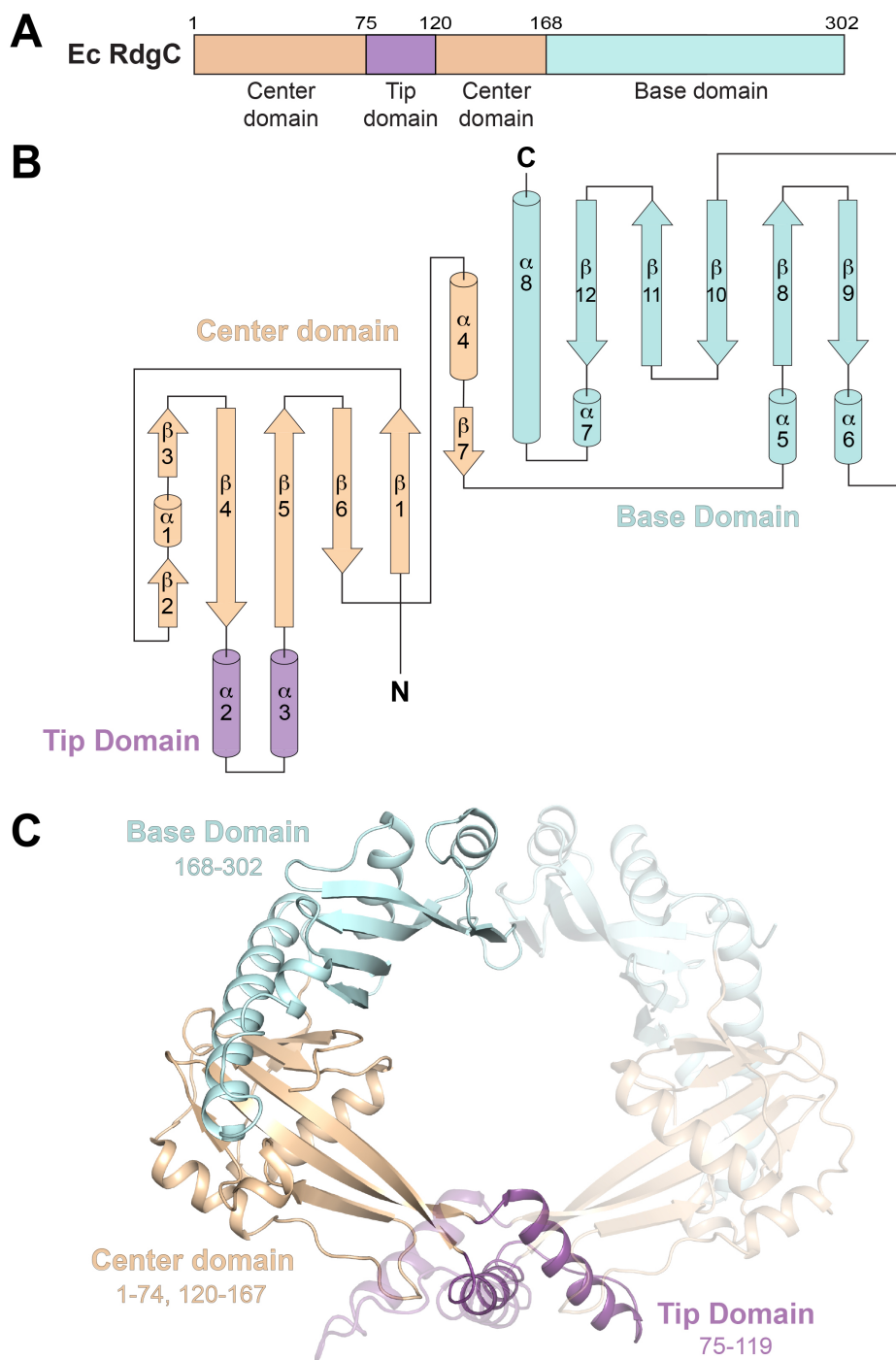
oligomerization of CI repressor molecules bound to the left and right operators results in stronger repression. Domain organization of CI is shown on the bottom right. B. Prophage induction and lytic activation. Cellular signals like DNA damage and the SOS response activate the RecA protein (RecA*), which promotes proteolytic cleavage of the CI repressor (5). This permits transcription from P_L and P_R lytic promoters. C. Model for RexA modulation of the λ bistable switch. In the absence of RexB, RexA can associate with both the CI repressor (by binding its CTD) and DNA. These protein–protein and protein–DNA interactions may destabilize CI repression and activate the lytic state (2).



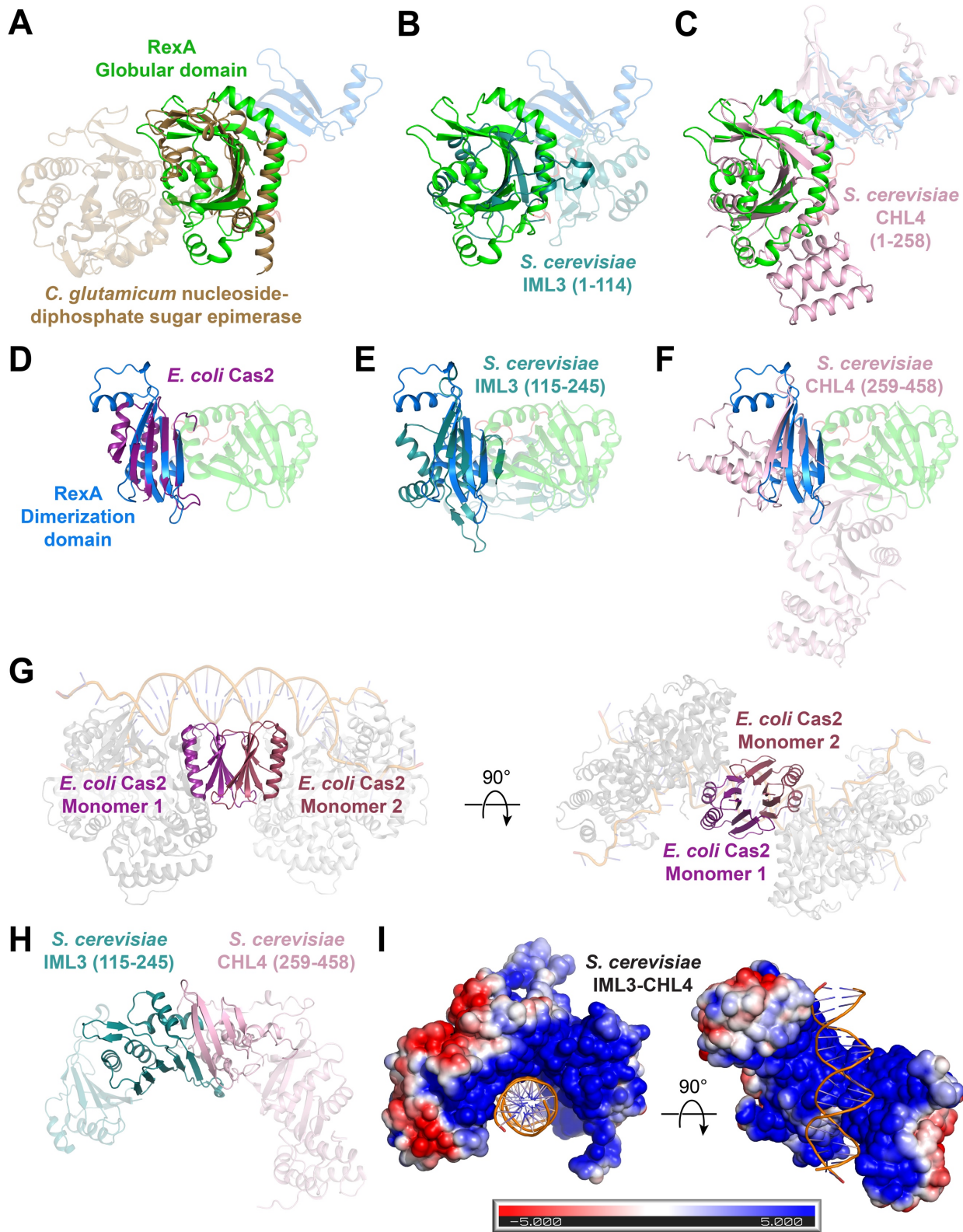
Supplementary Figure S2. Location of RexA mutants. A. Zoomed inserts denote locations of the D215 (blue) and residues 239-244 in the swivel loop (red) that are deleted in the $\Delta 239-244$ construct. Modeled D215W mutation (gray) is also shown, with red circles denoting expected steric clashes associated with this substitution. RexA monomers are colored in as in **Figure 1**. B. Location of R219 and K221 side chains in the dimerization domain.



Supplementary Figure S3. Structural coordination of bound ions and sulfates. A. Location of ordered sulfates (SO₄) and cadmium (Cd) ions associated with the RexA dimer following crystallization. Ions are numbered for reference (see B and C). RexA dimer is colored as in **Figure 1**. B. Zoomed views intramolecular ionic interactions. Interacting side chains are labeled with hydrogen bonds shown as dashed black lines. Superscripts "N" and "O" denote backbone nitrogen and carbonyl oxygens, respectively. Associated water molecules (red spheres) are shown where applicable. C. Zoomed views of intermolecular ionic interactions mediating crystal contacts. Symmetry-related molecules are colored gray.



Supplementary Figure S4. Structure and topology of *E. coli* RdgC. A. Domain architecture of *E. coli* (Ec) RdgC. B. Topology diagram of *E. coli* RdgC monomer with coloring as in B. C. Structure of *E. coli* RdgC dimer (PDB: 2OWL). The center, tip, and base domains are colored beige, purple, and cyan respectively in one monomer with accompanying residue numbering. Second monomer is colored the same but rendered partially transparent for contrast.



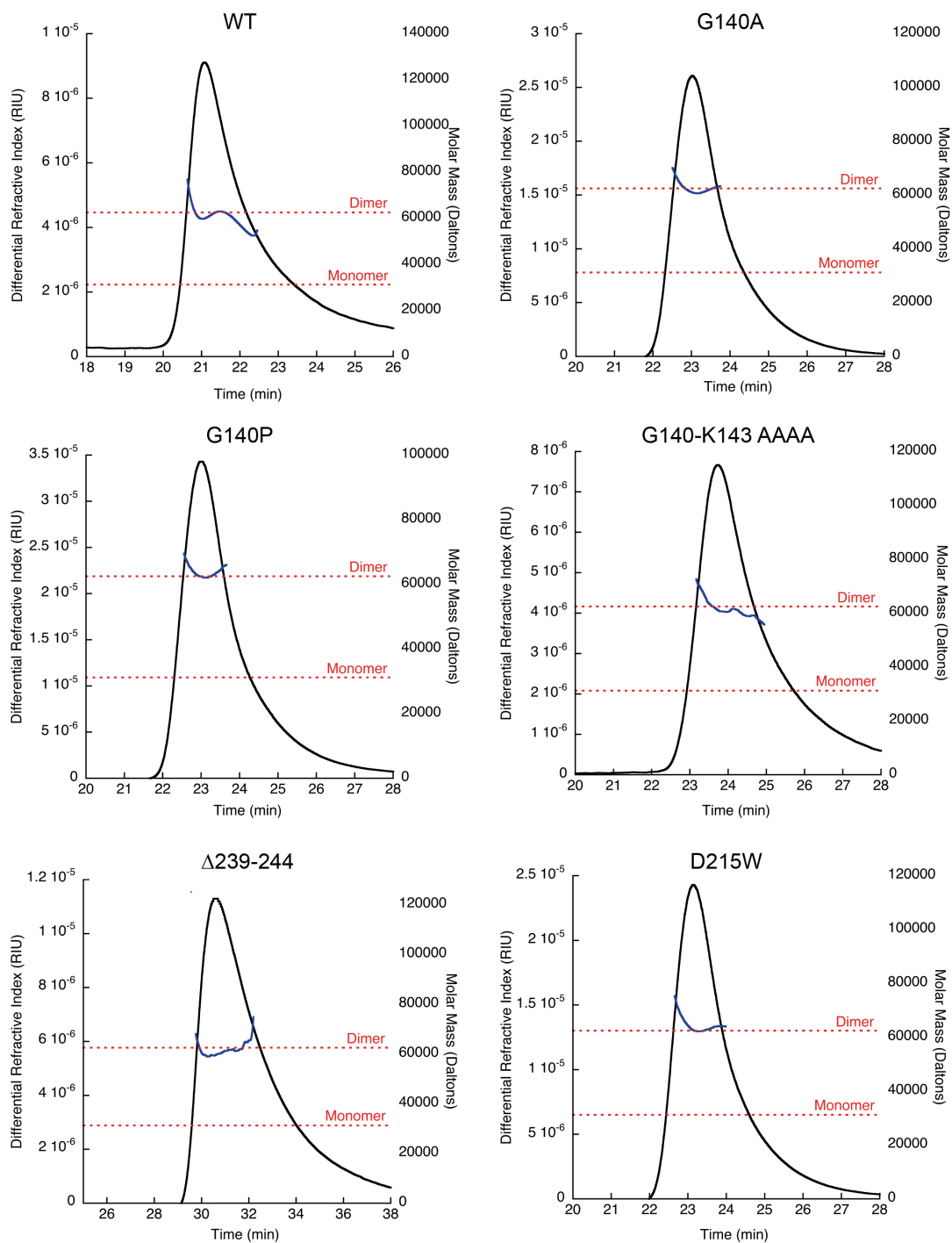
Supplementary Figure S5. Additional structural homologies identified by Dali. A-F, Superposition of λ RexA with a nucleoside-diphosphate sugar epimerase from *Corynebacterium glutamicum* (olive, PDB: 3OH8, Z-score 4.1, RMSD 4.4 Å), *Saccharomyces cerevisiae* IML3 (teal) and CHL4 (pink) (PDB: 8OVW, Z-score 4.1, RMSD 5.1 Å), and *E. coli* Cas2 (purple, PDB: 5DLJ, Z-score 4, RMSD 3 Å) illustrating structural homologies that are shared with RexA's globular (green) and dimerization (blue) domains, respectively. G. Orientation of Cas2 dimerization within Cas1-Cas2 dual-forked DNA complexes (PDB: 5DLJ) involved in CRISPR spacer acquisition. Cas 2 monomers are colored purple and ruby, respectively. H. The C-terminal segments of IML3 (teal) and CHL4 (pink) heterodimerize within the centromere-associated inner kinetochore (CCAN) complex (PDB: 8OVW) in a manner that creates an extend anti-parallel β -sheet across the dimer interface. I. Electrostatic surface of *Saccharomyces cerevisiae* IML3-CHL4 heterodimer. Scale bar indicates electrostatic surface coloring from $-5 K_bT/e_c$ to $+5 K_bT/e_c$. Centromeric DNA from the bound CANN complex (PDB: OVW) is shown.

BP λ. RexA		α3		β6		β7		α4		T.T													
		α3	TT	TT	β6	β7	TT	α4	T.T														
BP λ	68	INRSKA..	SVE	DIKNS	LAD	DESLGFP	SFL	FVEG..	DT	IGFAR	TVFGP	TTSDLT	FD	IGKGM	SLSS	.GER	VQ	133					
BPSfi	68	INRSKA..	SVE	DIKNS	LAD	DESLGFP	SFL	FVEG..	DT	IGFAR	TVFGP	TTSDLT	FD	IGKGM	SLSS	.GER	VQ	133					
Pbs	68	INRSKA..	SVE	DIKNS	LAD	DESLGFP	SFL	FVEG..	DT	IGFAR	TVFGP	TTSDLT	FD	IGKGM	SLSS	.GER	VQ	133					
EcK12	68	INRSKA..	SVE	DIKNS	LAD	DESLGFP	SFL	FVEG..	DT	IGFAR	TVFGP	TTSDLT	FD	IGKGM	SLSS	.GER	VQ	133					
Kp	68	INKSNA..	SVE	DIKSS	LAE	DESLGFP	SFI	FIDG..	DI	IGFAR	TIYGP	TTSDLT	FD	IGKGM	PADE	.GSRL	Q	133					
Cd	66	INKTKS..	SVE	DVKNS	LAD	DESLGFP	SFI	FMDG..	DV	IGFAR	TIYGP	TTSDLVD	FD	IGKGM	LVA	.GTX	IK	131					
Kl	68	IDRVNN..	NYQ	DIT	AL	QQNQ	VAF	ASYI	YISN..	RC	IGYGS	TLFGP	KVGS	FCKY	YDN	FFFN	NANN	.NRN	IR	133			
Ga	68	INTQDL..	SV	TEIQ	SIL	DK	DE	SIG	FSY	FI	KN..	NI	IGY	GP	TL	LSAK	INRF	YS	YI	132			
Seef	69	INKSQ..	SVE	DIKKS	LAA	DEVLGFP	SFI	YINK..	NT	IGFC	RTYGP	TIHDL	I	FL	IEKGL	NISE	.DSK	IT	134				
Er	69	INRSKS..	SVE	EIRKS	LAS	DESLGFP	SFI	YFDD..	SI	IGFAR	SMYGP	TTSDLT	IC	IL	SKEK	MP	PIPA	.STK	II	134			
Yr	70	INKSKA..	SVE	DIKGS	LAA	DESLGFP	SFV	FIDG..	DV	VGFAR	TMYP	TTSDLT	NF	VI	AKK	ITP	PI	.NST	VH	135			
Mo	69	INKKTS..	SIE	DIRKS	LAS	DESLGFP	SFL	FIND..	DV	IGFAS	TIYGP	SIRE	LKD	FL	CQK	IN	INND	.MT	LF	133			
Ec1	70	INRRTL..	SV	DIR	NAL	SS	DESLGFP	SFL	LIRK..	NI	IGYAN	TLFGP	KTRD	LAA	YI	KGK	GA	IPDG	.YS	LF	134		
Ko	70	INRRTL..	SV	DIR	NAL	SS	DESLGFP	SFL	QVRN..	NV	IGFAN	TLYGP	RTRD	LAS	YI	NGK	CY	IPSG	.YK	LV	134		
Op	70	INRRTL..	SV	DIR	NAL	SS	DESLGFP	SFL	IRE..	NV	IGFAN	TLYGP	RTKD	LTT	YI	ACK	Q	LP	SG	.RK	LV	134	
Ye	70	INRRTL..	SV	DIR	NAL	SS	DESLGFP	SFL	LIRK..	NV	IGFAN	TLYGP	RTKD	LNT	YI	SSK	G	ELDHG	.RK	LI	134		
Ia	68	VNKTTL..	SV	DEIK	NVL	GN	DE	TLA	FP	SFL	L	IKD..	GI	IGY	ACT	QHGP	R	VELE	I	Y	132		
Ec2	68	VNKTTL..	SV	DEIK	NVL	GN	DE	TLA	FP	SFL	L	IKD..	GI	IGY	ACT	QHGP	R	VELE	I	Y	132		
Seec	68	VNKTTF..	SID	EMK	NAL	GN	DE	TLA	FP	SFL	L	IKD..	NI	IGY	AS	SLHGP	R	TRDL	Q	Y	132		
Sees	120	VNKTTF..	SID	EMK	NAL	GN	DE	TLA	FP	SFL	L	IKD..	NI	IGY	AS	SLHGP	R	TRDL	Q	Y	132		
Cw	68	INRRTL..	SV	DEIK	NAL	GN	DE	TLA	FP	SFL	L	IKG..	NI	IGY	ACT	QHGP	R	TRDL	Q	Y	132		
Ae	70	INQNN..	SIND	I	RES	LAD	DE	ILG	FP	SFV	FIDN..	SIL	G	FV	TS	NWS	P	TR	E	FCD	Y	134	
Pm2	70	INQNN..	SIND	I	RES	LAD	DE	ILG	FP	SFV	FIDN..	SIL	G	FV	TS	NWS	P	TR	E	FCD	Y	134	
Pm1	70	INQNN..	SIND	I	RES	LAD	DE	ILG	FP	SFV	FIDN..	SIL	G	FV	TS	NWS	P	TR	E	FCD	Y	134	
Mm	70	INQNN..	SIND	I	RES	LAD	DE	ILG	FP	SFV	FIDN..	SIL	G	FV	TS	NWS	P	TR	E	FCD	Y	134	
Pc	70	INRSNS..	SV	KDIR	DS	L	TE	DE	SLG	FP	SFI	FIDG..	NV	M	G	FAS	SMYGP	R	REL	A	E	135	
Xb	68	INTSTF..	SV	ANIR	DS	L	AS	DE	SLG	FP	SFI	FIDG..	NV	M	G	FAS	SMYGP	R	REL	A	E	135	
As	75	INENSI..	SV	GDIK	DK	L	HNN	E	KV	A	F	TS	HI	L	SS	DR	S	L	A	I	AS	143	
Vm	75	VNEQDI..	TV	SE	IS	EN	L	AAN	E	KV	A	F	TS	HI	L	SS	DR	S	L	A	I	AS	143
Fa	73	IERATL..	KH	E	D	L	ST	K	G	T	A	N	S	V	G	M	A	S	Y	V	K	E	138
Wc1	74	INSSKL..	T	I	E	D	I	K	A	T	F	N	P	E	K	L	G	F	S	Y	I	Y	139
Wc3	73	IDNSSL..	T	I	E	D	I	R	E	T	L	K	D	E	N	L	G	F	S	Y	I	Y	139
Ig	94	IQTKNL..	E	I	K	D	E	S	Q	L	S	D	G	E	K	I	G	Y	S	S	V	F	138
Wc2	86	IDKEEL..	T	V	S	D	I	K	E	K	L	Q	A	E	S	I	A	F	A	A	Y	F	138
Sk	73	INSECF..	T	Y	E	D	I	R	D	D	L	D	N	E	K	V	F	A	S	Y	V	I	151
Ab	80	IERSEKEI	K	A	H	E	I	Q	S	L	L	S	K	D	E	S	L	G	F	A	S	Y	150
Sa	73	IQSQDF..	SV	SE	I	G	A	M	L	R	A	G	E	L	G	F	A	S	Y	I	Y	V	139
Ap	73	IKSSDL..	SV	TE	I	Y	D	L	S	A	D	E	L	G	F	A	S	Y	I	Y	V	139	
Ha	73	IKSTDH..	SV	SE	I	N	D	M	L	Q	R	D	E	R	L	G	F	A	S	Y	I	Y	139
Gm	73	VNPNNV..	SV	GE	I	N	S	L	E	Q	D	E	L	G	F	A	S	Y	I	Y	V	139	
Pf	77	INTSNF..	S	I	S	E	V	R	K	I	L	G	A	D	E	K	I	G	F	A	S	Y	143
Ps	73	INTANL..	S	I	S	E	I	R	S	M	L	G	S	E	E	K	I	G	F	A	S	Y	139

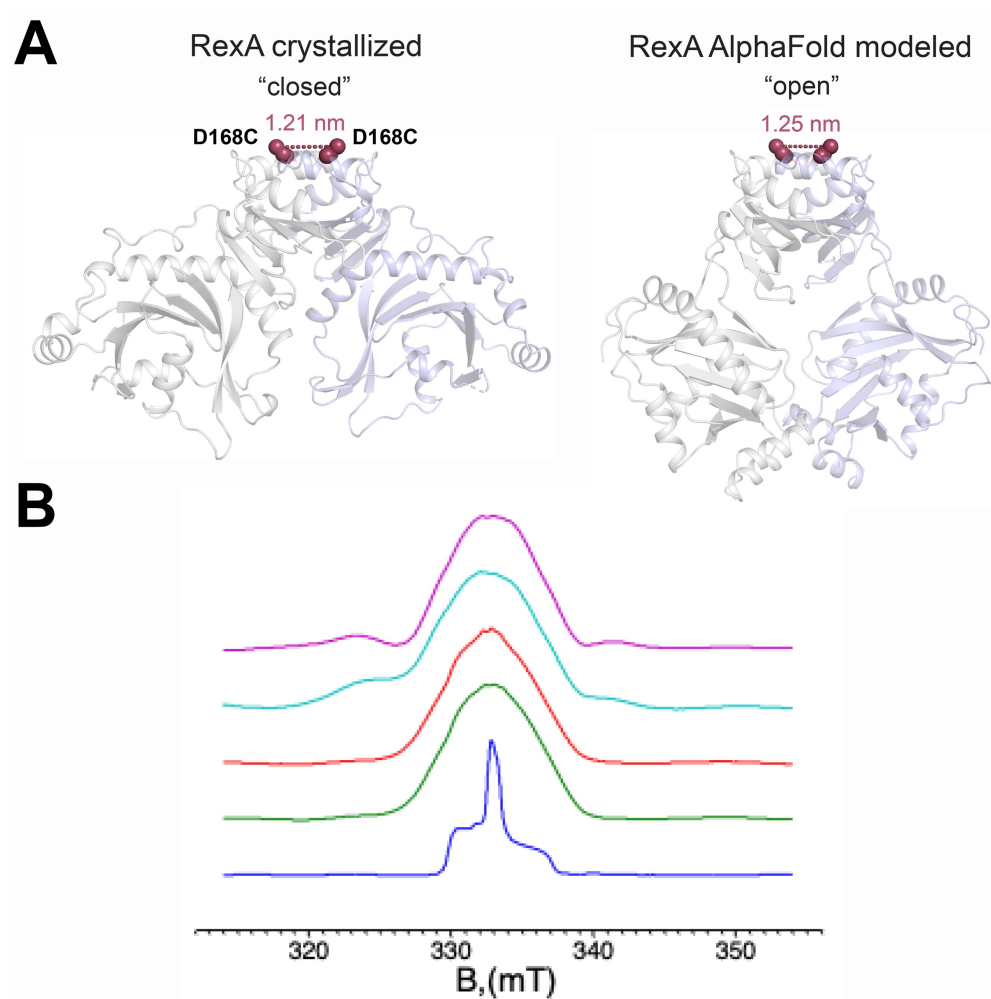
BP λ. RexA		β8		α5		β9		α6		η1		β10		TT																		
				ℓℓℓℓ				ℓ...ℓℓℓℓℓ...ℓℓ		ℓℓℓ																						
BP λ	134	IE	PLMRGT	TKD	DVM	HH	FIGR	TTV	KVEAK	LP	...	VFGD	IL	...	KV	LGATD	...	IEG	EL	FDS	LDIV	IKPK	FK	195								
BPSfi	134	IE	PLMRGT	TKD	DVM	HH	FIGR	TTV	KVEAK	LP	...	VFGD	IL	...	KV	LGATD	...	IEG	EL	FDS	LDIV	IKPK	FK	195								
Pbs	134	IE	PLMRGT	TKD	DVM	HH	FIGR	TTV	KVEAK	LP	...	VFGD	IL	...	KV	LGATD	...	IEG	EL	FDS	LDIV	IKPK	FK	195								
EcK12	134	IE	PLMRGT	TKD	DVM	HH	FIGR	TTV	KVEAK	LP	...	VFGD	IL	...	KV	LGATD	...	IEG	EL	FDS	LDIV	IKPK	FK	195								
Kp	134	VE	PLMRGT	TKD	DVM	SMH	FIGR	TTV	KVEAK	SS	...	AFGD	IL	...	KT	LGAKD	...	IEG	EL	FDS	IEIV	IKPK	FK	195								
Cd	132	IE	PLMRGT	SKG	DVM	KMN	FIGR	TTV	KVEAK	ST	...	TFGD	IL	...	KT	LGAKD	...	IEG	EL	FDS	IEIV	IKPK	FK	193								
Kl	134	VE	PI	SKT	VT	PAQ	AL	QFA	H	MGR	I	N	V	K	L	E	P	N	S	...	F	A	L	R	EMT	195						
Ga	133	FEP	ICK	N	VT	AET	A	M	K	L	E	F	I	G	K	T	I	K	V	E	A	K	S	...	191							
Seef	135	LE	PIMRST	TKED	DVM	KMY	YIGR	TTV	KVEAG	TG	...	IFNG	IL	...	NFL	GAKA	...	IEG	EL	FDS	LEVI	IKPK	Y	196								
Er	135	VE	PLMRGT	TKA	D	V	Q	K	M	H	FIGR	TTV	K	V	E	A	G	T	...	L	S	E	G	I	L	...	196					
Yr	136	IE	ALMRGT	TEA	D	V	M	A	M	Q	FIGR	TTV	K	V	E	A	G	T	...	V	F	D	G	V	...	197						
Mo	134	FEP	LIR	N	I	S	S	K	E	T	E	K	M	V	FIGR	T	T	L	K	T	E	A	D	...	195							
Ec1	135	IE	PLMRDI	TKD	D	A	L	S	M	Q	FIGR	TTV	R	V	E	N	G	S	...	L	F	S	P	L	L	...	196					
Ko	135	IE	PLMRDI	TKD	D	A	L	S	M	Q	FIGR	TTV	R	V	E	N	G	S	...	L	F	S	P	L	L	...	196					
Op	135	IE	PLMRDV	SKS	D	A	L	D	M	E	FIGR	T	T	L	R	V	E	S	G	...	L	F	S	P	L	L	...	196				
Ye	135	IE	ALMRDV	TKT	E	A	L	D	M	E	FIGR	T	T	L	R	V	E	S	G	...	L	F	S	P	L	L	...	196				
Ia	133	LGPL	MRDV	TKD	D	A	L	D	M	E	FIGR	T	T	L	R	V	E	S	G	...	L	F	S	P	L	L	...	194				
Ec2	133	LE	PLMRDV	TRD	D	A	L	D	M	E	FIGR	T	T	L	R	V	E	S	G	...	L	F	S	P	L	L	...	194				
Seec	133	IE	PLMRDV	SKD	D	A	L	E	M	Q	FIGR	T	T	L	R	V	E	S	G	...	L	F	S	P	L	L	...	194				
Sees	185	IE	PLMRDV	SKD	D	A	L	E	M	Q	FIGR	T	T	L	R	V	E	S	G	...	L	F	S	P	L	L	...	194				
Cw	133	IE	PLMRDL	SKD	D	A	L	G	M	Q	FIGR	T	T	L	R	V	E	S	G	...	L	F	S	P	L	L	...	194				
Ae	135	VE	PLMQGI	TKV	D	A	L	N	M	N	FIGR	T	T	L	R	I	E	S	G	...	L	T	N	I	L	...	196					
Pm2	135	LE	PLMKGT	SKN	D	A	L	K	M	N	FIGR	T	T	L	R	V	E	S	G	...	L	T	R	A	L	L	...	196				
Pm1	135	VE	PLMRGV	TKA	D	A	L	N	M	S	FIGR	T	T	L	R	I	E	S	G	...	L	T	K	T	I	...	196					
Mm	135	VE	PLMKWV	TKA	D	A	L	N	M	T	FIGR	T	T	L	R	I	E	S	D	K	...	M	M	K	T	L	...	196				
Pc	136	AE	PLMRDM	SKD	D	A	L	K	M	D	FIGR	T	T	L	R	V	E	T	G	N	...	I	C	S	E	I	...	197				
Xb	131	IE	PLMQNV	T	T	E	D	A	L	T	M	Q	FIGR	T	T	L	R	V	E	S	D	...	G	R	G	A	T	195				
As	144	FTAL	T	S	N	A	T	K	K	D	L	E	M	E	V	N	S	I	F	V	D	V	A	D	N	...	203					
Vm	144	LSAL	T	T	I	S	S	K	D	L	E	M	E	V	N	S	I	F	V	D	A	D	R	...	203							
Fa	139	LAAPND	K	V	S	K	K	D	I	V	K	L	N	H	V	S	S	I	G	L	N	A	S	...	201							
Wc1	140	LEA	I	M	T	E	L	S	A	A	D	A	K	K	L	A	F	V	S	R	A	H	I	K	V	P	202					
Wc3	139	AE	PL	L	T	S	L	T	K	D	E	A	K	S	L	A	F	I	S	R	A	V	K	V	P	Q	R	201				
Ig	160	V	T	P	Q	I	D	L	H	Q	S	E	V	D	D	L	S	P	I	G	T	G	S	V	E	I	221					
Wc2	152	V	T	I	M	A	E	Q	T	S	I	H	E	A	L	T	D	F	I	G	R	T	I	E	A	S	219					
Sk	139	A	T	P	P	P	V	Q	S	S	D	V	M	T	M	N	S	V	G	R	T	T	F	E	V	S	198					
Ab	151	IHP	L	L	T	K	L	T	K	K	Q	A	M	N	F	I	G	T	R	I	O	I	D	G	N	S	...	194				
Sa	140	LM	PLL	Q	S	T	R	E	V	L	S	M	S	V	G	R	S	S	O	I	N	K	E	S	...	201						
Ap	140	LN	PLL	T	Q	S	T	K	A	D	A	M	K	D	FIGR	S	V	I	O	T	K	E	N	S	...	201						
Ga	140	LHP	F	M	Q	E	A	T	F	A	D	A	L	M	Y	FIGR	S	S	V	O	K	E	N	S	...	201						
Hm	140	Q	P	A	L	L	Y	Q	A	T	K	E	A	L	S	P	H	I	G	R	T	T	I	E	L	S	K	N	S	...	201	
Pf	144	I	S	P	L	I	K	Q	A	T	K	E	A	V	S	M	E	Y	I	G	R	T	T	I	E	V	T	R	N	S	...	204
Fs	140	I	T	PL	L	Q	A	T	K	S	A	V	M	E	Y	I	G	R	T	T	I	E	V	G	R	K	N	T	...	204		

Supplementary Figure S6. Sequence alignment of putative RexA homologs. Sequence alignment of RexA homologs with the secondary structure of the bacteriophage λ RexA mapped above. Colored bars beneath the alignment denote structural segments as follows: globular domain, green; dimerization domain, blue; hinge loop, magenta; swivel loop, red (see **Figure 1**). Positions of conformational mutations are marked below (see **Figures 4 and 5, Supplementary Figure S2**). Red text bounded by blue border denotes 70% sequence conservation. Abbreviations are as follows with accompanying NCBI accession numbers or KEGG IDs (6) : BP λ , bacteriophage λ RexA (vg:3827058); BPSfl, bacteriophage Sfl gp47 (vg:24722216); Pbs, *Paenibacillus sonchi* (pson:J1735_34930), EcK12, *Escherichia coli* K-12 BW2952 (ebw:BWG_3702), Kp, *Klebsiella pneumoniae* (WP_117261707.1); Cd, *Cedecea davisae* (WP_202303730.1); Kl, *Klebsiella multispecies* (WP_071995728.1); Ga, *Gilliamella apicola* (WP_065635067.1); Seef, *Salmonella enterica* subsp. *enterica* FNW19H96 (EDW1732907.1); Er, *Erwinia* sp. S38 (WP_200545456.1); Yr, *Yersinia ruckeri* (WP_234057212.1); Mo, *Morganellaceae* multispecies (WP_154640079.1); Ec1, *Escherichia coli* (WP_253764069.1); Ko, unclassified *Kosakonia* multispecies (WP_200133690.1); Op, *Obesumbacterium proteus* (WP_234559868.1); Ye, *Yersinia enterocolitica* (WP_050128085.1); Ia, *Izhakiella australiensis* (WP_096777782.1); Ec2, *Escherichia coli* (WP_197940034.1); Seec, *Salmonella enterica* subsp. *enterica* serovar Cubana (seec:CFSAN002050_11670); Sees, *Salmonella enterica* subsp. *enterica* serovar Saintpaul (ECA2934630.1); Cw, *Citrobacter werkmanii* (WP_085048607.1); Ae, *Arsenophonus* endosymbiont of *Apis mellifera* (aet:LDL57_11880); Pm2, *Proteus mirabilis* (WP_143474652.1); Pm1, *Proteus mirabilis* (WP_206081156.1); Mm, *Morganella morganii* (WP_049246396.1); Pc, *Photorhabdus cinerea* (WP_166310405.1); Xb, *Xenorhabdus bovienii* (WP_038244014.1); As, *Alteromonas stellipolaris* R10SW13 (aaw:AVL56_04330); Vm, *Vibrio mimicus* (vmi:AL543_00300); Fa, *Frateuria aurantia* (fau:Fraau_1963); Wc1, *Wohlfahrtiimonas chitiniclastica* (WP_213398763.1); Wc3, *Wohlfahrtiimonas chitiniclastica* (WP_094493134.1); Ig, *Ignatzschineria* sp. HR5S32 (ign:MMG00_12050); Wc2, *Wohlfahrtiimonas chitiniclastica* (WP_213405574.1); Sk, *Shewanella khirikhana* (skh:STH12_00053); Ab, *Acinetobacter baumannii* BJAB0715 (abab:BJAB0715_02483); Sa, *Salinisphaera* sp. (MBS61511.1); Ap, *Abyssibacter profundus* (WP_109719971.1); Ha, *Halomonas* sp. 3F2F (WP_226930571.1); Gm, *Gallaecimonas mangrovi*

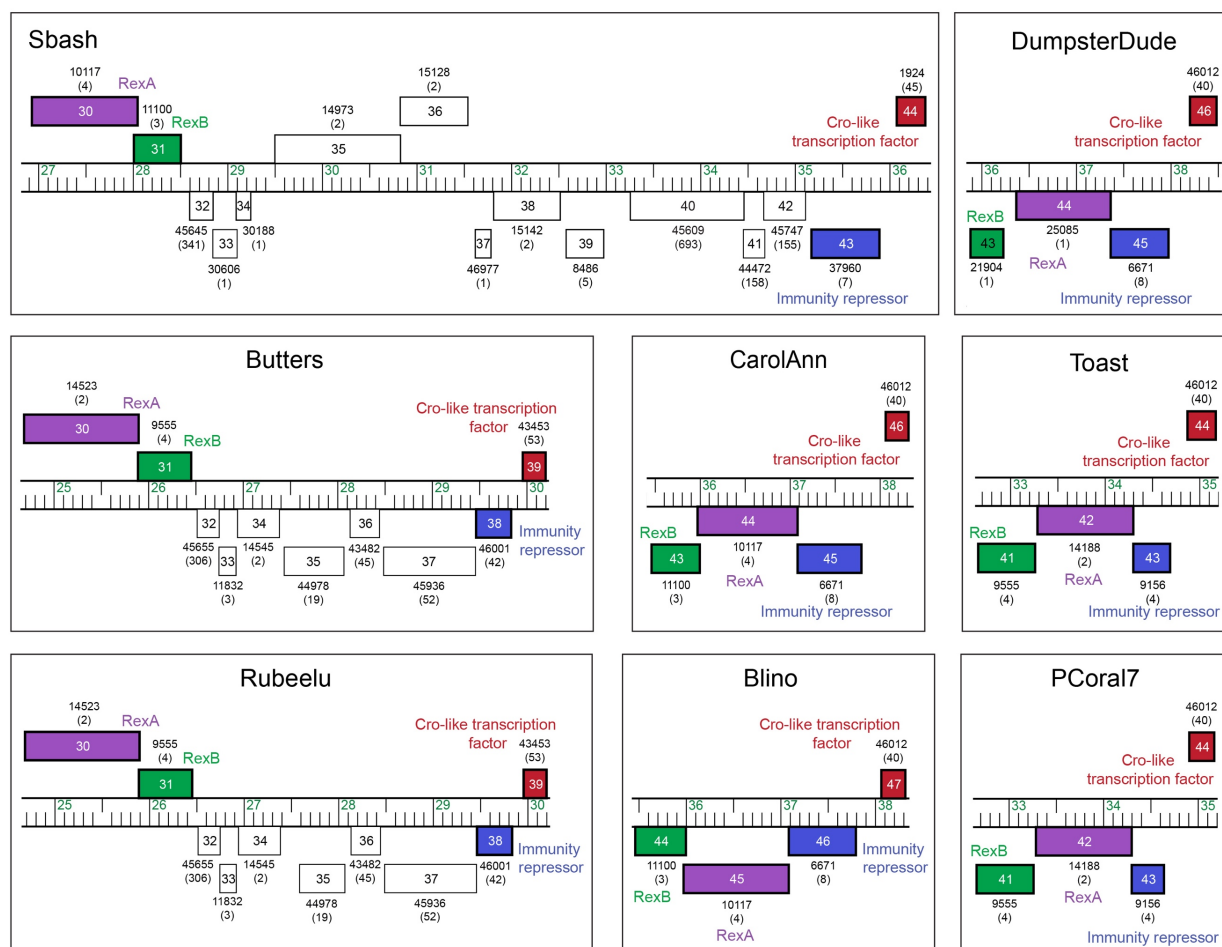
(WP_115720386.1); Pf, *Pseudomonas fragi* (pfz:AV641_12615); Ps, *Pseudomonas syringae* (WP_198722127.1).



Supplementary Figure S7. SEC-MALS analysis of RexA mutants. Black line denotes differential refractive index and blue line denotes measured mass across each peak. Dashed red lines indicate the predicted molecular weight of a RexA monomer and dimer.



Supplementary Figure S8. ESR spectroscopy measurements for D168C. A. Predicted distances between the D168C substitutions (red spheres) in the crystallized (closed) and AlphaFold modeled (open) RexA dimer structures. B, Integrated CW-ESR spectra of D168C (green); D168C/DNA (red); D168C/D215W (cyan); and D168C/D215W/DNA (magenta) spin-labeled RexA mutants. The rigid-limit unbroader nitroxide spectrum (blue) was plotted as a reference. All D168C spectra show large dipolar broadening ~ 2 mT corresponding to ~ 1 nm distance between spin labels. Spectral features caused by nitroxide labels not having partners were subtracted out. There is no visible effect of DNA but D215W mutation adds shoulders to the spectra.



Supplementary Figure S9. Gene neighborhoods surrounding RexA-like genes in Actinobacteriophages. Genomic organization around RexA-like genes in Sbash, DumpsterDude, Butters, Rebeelu, CarolAnn, Blino, Toast, and PCoral7 phages generated via Phamerator (7). Individual genes are depicted as boxes with the gene name inside the box and the Pham family designation and number of Pham members (in parentheses) shown below each box. Genes corresponding to RexA (purple), RexB (green), a CI-like immunity repressor (blue), and Cro-like transcription factor (red) are colored and labeled.

```

λ RexA      1 : -----MKNGFYATYRSKNKGKDKRSINISVFLNSLLADNH-HLQVGSNYLYIHKIDG-----KTFLFTKTNDSKSLVQKINRSK : 72
Sbash gp30 1 : -----MTGERQIVAYGGRVEVDGGAQRRTKNPPHTPYPANFNGAGADLLMFFSSFNALPTD----- : 58
CarolAnn gp44 1 : -----MGTWGDRIIVLYTIRVALDGRVFTS--AAAGEFFVANFNNGSCADLLHFLSSFEALPTD----- : 58
Toast gp42 1 : -----PSYGRHFYKVELFNGNK----QTPLSFIE-EDCGKSWRYGE-HIATYLE----- : 44
DumpsterDude gp44 1 : -----MPRRTITVTEVWAHPVG--SRKE--KDRVDTALPDGMDLLHAFYGAADVDAR----- : 50
Butters gp30 1 : MLWDRTSHVLSISYANLRTSTHPLLTNNGFRLIQVGVYRNGR--GDPCAVDA--ICDDKQHFDR-KTFDLAN----- : 66

λ RexA      73 : ASVEDIKNSLADDESLEFESFLFVEGDTGFARTV-----FGPTTSDLTDFLIGKMSLSSGER : 131
Sbash gp30 59 : -----KLIRRGDRHFGIEEVEVERLGRIT-----RLRISGGESGRRSKIT----- : 97
CarolAnn gp44 59 : -----KHIERDERHFGQETSIRRRGRIT-----SWRDGGESGRRSQIR----- : 97
Toast gp42 45 : -----RFKENQVRGEPERSQTPDESSVDQ-----IRKKTAVVFNADVRRGPNVVAEYRVGRSDDFDR-- : 101
DumpsterDude gp44 51 : -----QLLKENESFASVVSLEEKGRV-----TLAVDVGRFGERGTIT----- : 85
Butters gp30 69 : -----RKKDCVVHSGSPRSKEEGSDDESADVDHESVDDDAEQQTGAKRPRPVIVITDVSFGD-HVVEIYLYGRDLGYTH-- : 144

λ RexA      132 : VQIEPLMRGTTKDDVMHMHFIGRTTVKVEAKLVFVGDKLVKLCATDFEGELFDSL---DIVIKPKKKDIKKVAKDIIF----- : 207
Sbash gp30 98 : -----LKAGGKEETREPSGVWEPPFVAIVLKKDFNQ---GWLVEKSGYHSV---PTEWRQELVRAFKAAAYPDYVL-KISSITEM : 171
CarolAnn gp44 98 : -----LRRDADAQERDRSGVEWEPFVAFVAVVENSVV---GWLVEKAGRHSL---PTEWRKELOQFAGAYRGYRL-EIGIVREM : 171
Toast gp42 102 : --AYPAPDLETSDYLELNGYAPARPYRAVLMVPEGEV---GMLAVEAIGRTCPYEFFTKWATKWSVDYQALD---SSDPLDDDKV : 180
DumpsterDude gp44 90 : -----DVTTMIERDRFRTDAISVITHGIFTLPKGTCS---ALVFIERSGNOSG---IIRVLELQHQERLAYPDLL-ETTAVVES : 164
Butters gp30 145 : --AGYSEQDTTAKAVRIANLKSVRPYSVFMFEDVGNS---GVVAVEDASRAHASKLEQWLKAWAEAEAHVAEIKRKETGKKSIK : 226

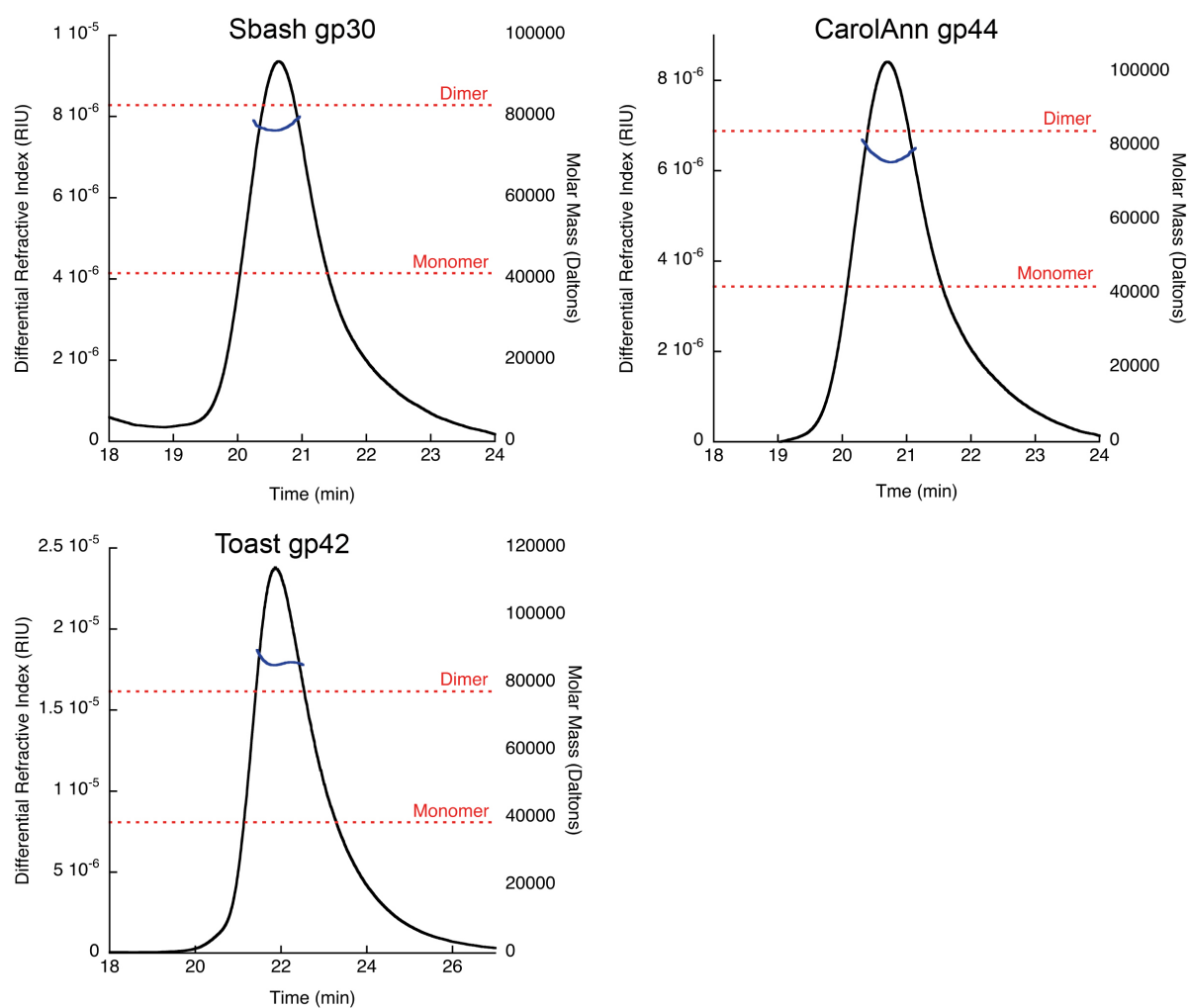
λ RexA      208 : -----NPSPPQFSDISIRAKDEA---GDILTEHYLSEKGLHS--APLN-----KVTNAEIAEEM--ACYARMK----- : 263
Sbash gp30 172 : SLISQVE--NSN-EPRLTAVEVIMRSS---DSSGDHSAAGHPANMATYDTHVWEAVHAQPG--RVLSQILRRRTRRKTK---DGL--- : 244
CarolAnn gp44 172 : SLIAQVE--NALDEERLIGFEVAYRSA---STTAGSGAAGYERGMKYERRMWRAPADQPKKGRKLREFRRAHT-KTLI---EGT--- : 247
Toast gp42 181 : RAVWRLLKPTPLGSKSQLVDFIKGKTIEELILINHVIDKTRNER-QERFR-----VKAKVETGQRPYAKKRLNEV---FEV : 251
DumpsterDude gp44 165 : EALISYA-----SLVKVSAHRA-----SGSDEA--DNNSKRIKSEYGEAHLTVFARGETLPR--LYDRLV---AGA--- : 228
Butters gp30 227 : PVVWSMRFTPLSDPERLAALMKNGTSSKIVLTKQGGSDDARTPG-RSLPK---VEMGLDEPASIAKARLRITGLPKFNRTPOAGDAQV : 310

λ RexA      264 : -----SDILECFRQVGKVID----- : 275
Sbash gp30 245 : -----VEITQPLDVDDLSDDAKIELRDDVRCIARVLNSEGRKKTIVFEGGRE-PTMTIVMDGVFDLSPSATKFWQEARSA--- : 315
CarolAnn gp44 248 : -----REIELPFEADLSDDRYTIIRLRDDVAEIRATLYNSEGPKTVVFEGLD-PQQTIVMEDTALAPPDQDRFDETCRSA--- : 322
Toast gp42 252 : DSDEVFARQLAENFGNSVEHLDDGGVYVVEA-GVNIS--PSRMPEVFTYFVSD-----DR--PT-MEEELTAV----- : 317
DumpsterDude gp44 229 : -----LKPSELLDFDE-SDE-----AAHVE-VTLEHNGQRKTFLLGHEKRPISYLL-----SNHGEDEWSLERVRDYA : 290
Butters gp30 311 : AANRELAAVLADNYQ-GFDEEDYDDAWIEVDAAGKAKKIS--PSRWADIFIYFVRN-----STECPP-PALFYRRV----- : 378

λ RexA      - : ----- : -
Sbash gp30 320 : ---VVDIATSGGVSLAPKWDITGEIEHPENAIKVEVSLTDEPDQDDAASAGGTGTTA : 372
CarolAnn gp44 323 : ---VRDIAASNVMGLAPKWDITGDIHVPEDAVKLEVKSDAPSPERDQGSEAN----- : 370
Toast gp42 318 : --KRHAIPAKVID---AQVDFDS----- : 337
DumpsterDude gp44 291 : FDTHADTYGRLGWEWTPAHTVGAWTDSQGARLVVRGGEQS----- : 332
Butters gp30 379 : -QESVRPEKSLE---LSIDWAGGGDSG----- : 403

```

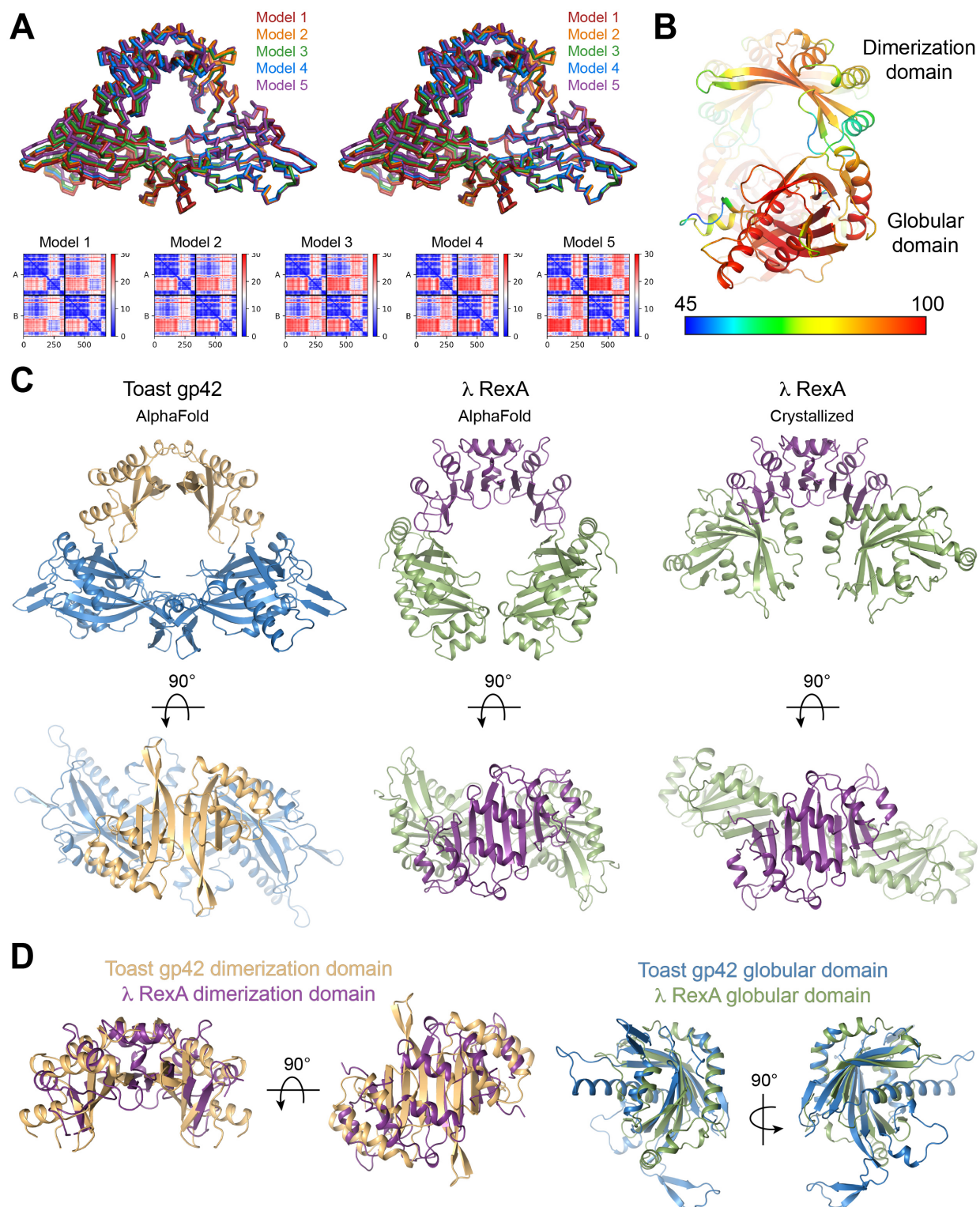
Supplementary Figure S10. Sequence alignment of unique RexA-like proteins present in Actinobacteriophage viruses. Alignment includes unique RexA homologs present in the Actinobacteriophage Database (PhagesDB) (8). Sequences for Blino gp45, PCoral7 gp42, and Rebeelu gp30 are omitted as they are each 100% identical to CarolAnn gp44, Toast gp42, and Butters gp30, respectively. Sequence shading indicates conservation: white text on black background, 100% conserved; white text on dark gray background, 80% conserved; black text on light gray background, 60% conserved.



Supplementary Figure S11. SEC-MALS analysis of purified RexA homologs. Black line denotes differential refractive index and blue line denotes measured mass across each peak. Dashed red lines indicate the predicted molecular weight of a monomer and dimer for each homolog.

	OR3	OR2	OR1
λ :	TATCACCGCAAGGGATAAATATCTAACACCGTGCCTGTTGACTAT---	TTTACCTCTGGCGGTGATA	
CarolAnn :	CATACACGCAGGCTGCGGAACCTACCGCCGTGTAATTCAATTGCCATGCGTGTACCCACCATGCAAGAA		
Toast :	CATATCCGCAGGCTGCGGAACCTACAGGGCTGTAATTTCTTGACGAGCGTCTACCTGCTGCGGAAGAA		
Sbash :	CTTTCGAACCTGGGTGGCAAACATCATCAGTGTAAATTCCTCCGACTATTGGGTCTTAGGTCAAGAAA		

Supplementary Figure S12. Comparison of operator sequences used in binding experiments. Alignment of the genomic region encompassing the operator sites O_{R1} , O_{R2} , and O_{R3} in phages λ , CarolAnn, Toast, and Sbash. Sequence shading indicates conservation: white text on black background, 100% conserved; white text on dark gray background, 80% conserved; black text on light gray background, 60% conserved. DNA substrates containing λ O_{R1} and O_{R2} were used for EMSAs, limited proteolysis, and ESR experiments (**Figures 4, 5, and 7**) while substrates containing O_{R1} , O_{R2} , and O_{R3} were only used for EMSAs with individual RexA homologs (**Figure 7C**). See **Supplementary Table S2** for sequences of each individual substrate.



Supplementary Figure S13. AlphaFold model of Toast gp42 and comparison to RexA. A. Superposition of top 5 Toast gp42 models generated with AlphaFold-Multimer (9) viewed in

stereo. Predicted aligned error plots are shown below. B. Side view of Toast gp42 model colored according to the predicted local distance difference test (pLDDT) score (0-100), with values greater than 90 indicating high confidence and values below 50 indicating low confidence. Scale bar denotes per residue confidence coloring for pLDDT scores ranging from 45 to 100. C. Comparison of Toast gp42 AlphaFold model (left) with the RexA AlphaFold model (center, predicted open conformation) and crystallized RexA structure (right, closed conformation). Side and top views are shown for each. Coloring as follows: Toast gp42 dimerization domains, light orange; Toast gp42 globular domains, sky blue; RexA dimerization domains, violet purple; RexA globular domains, smudge. D. Superposition of the dimerization domains (left) and individual globular domains (right) from the Toast gp42 AlphaFold model and the crystallized RexA coordinates.

SUPPLEMENTARY REFERENCES

1. Thomason,L.C., Morrill,K., Murray,G., Court,C., Shafer,B., Schneider,T.D. and Court,D.L. (2019) Elements in the λ immunity region regulate phage development: beyond the 'Genetic Switch.' *Mol Microbiol*, **112**, 1798–1813.
2. Thomason,L.C., Schiltz,C.J., Court,C., Hosford,C.J., Adams,M.C., Chappie,J.S. and Court,D.L. (2021) Bacteriophage λ RexA and RexB functions assist the transition from lysogeny to lytic growth. *Mol Microbiol*, **116**, 1044-1063.
3. Hochschild,A. and Lewis,M. (2009) The bacteriophage λ CI protein finds an asymmetric solution. *Curr Opin Struc Biol*, **19**, 79–86.
4. Oppenheim,A.B., Kobilier,O., Stavans,J., Court,D.L. and Adhya,S. (2005) Switches in bacteriophage lambda development. *Annu Rev Genet*, **39**, 409–429.
5. Casjens,S.R. and Hendrix,R.W. (2015) Bacteriophage lambda: Early pioneer and still relevant. *Virology*, **479**, 310–330.
6. Kanehisa,M., Furumichi,M., Tanabe,M., Sato,Y. and Morishima,K. (2017) KEGG: new perspectives on genomes, pathways, diseases and drugs. *Nucleic Acids Res*, **45**, D353–D361.
7. Cresawn,S.G., Bogel,M., Day,N., Jacobs-Sera,D., Hendrix,R.W. and Hatfull,G.F. (2011) Phamerator: a bioinformatic tool for comparative bacteriophage genomics. *Bmc Bioinformatics*, **12**, 395.
8. Russell,D.A. and Hatfull,G.F. (2016) PhagesDB: the actinobacteriophage database. *Bioinformatics*, **33**, 784–786.
9. Evans,R., O'Neill,M., Pritzel,A., Antropova,N., Senior,A., Green,T., Žídek,A., Bates,R., Blackwell,S., Yim,J., *et al.* (2022) Protein complex prediction with AlphaFold-Multimer. *Biorxiv*, 10.1101/2021.10.04.463034.